



10-6-9

STUDY ON 3-D MODAL MODELING OF BOILER STRUCTURES USING SEISMIC AND MICROTREMOR RECORDS

Eiichi NISHIDA¹, Masakatsu IMAMURA² and Tatsuo KIRIYAMA²

1 Kure Research Laboratory, Babcock-Hitachi K.K.
Kure, Hiroshima, Japan

2 Thermal Power Design Dept., Babcock-Hitachi K.K.
Kure, Hiroshima, Japan

SUMMARY

This paper deals with the study of base excitation modeling by modal analysis which is based on a multi-input/output system identification method. At first, the application method of multi-point random excitation techniques and curve-fit algorithms for force excitation data to base excitation data, is studied. Furthermore, this method is applied to the microtremor records of boiler plant structures in thermal power stations. The identified modal parameters are shown to be in good agreement with those of FEM. As a result of these investigations, this kind of modal analysis has proven to be an effective tool for seismic modeling of large scale structures.

INTRODUCTION

In present day experimental modal analysis, multi-input/output system identification methods have been adopted using multi-point force excitation techniques (Ref. 1). But most of these methods can not utilize base excitation data such as seismic or microtremor records. This paper deals with the study of the application method of modal analysis mentioned above, to base excitation data. Here, taking into account multi-directional base acceleration data, base excited structures are regarded as multi-input/output systems.

This method is applied to the microtremor records of boiler plants in thermal power stations in order to achieve there seismic modeling. The boiler plant has an asymmetrical structure, so, there will be coupling modes in two horizontal directions. Besides that, FEM simulation suggests high modal density ; 7 or 8 modes in 1 ~ 3 Hz. Considering these vibration characteristics of the boiler plant, modal identification was achieved and the results were compared with those of FEM.

APPLICATION METHOD OF MULTI I/O MODAL ANALYSIS

The process of modal analysis is composed of two stages ; calculation of frequency response functions (abbr. FRFs) and curve-fittings of them to extract modal parameters. Recently, multi I/O type curve-fit algorithms (abbr. poly-reference methods) have been developed for force excitation systems (Ref. 2). They process simultaneously the group of FRFs which have multi-input (or multi-reference). As a result of the comparative study between the equations of FRF for force excitation systems and that of base excitation systems, any type of curve-fitting methods developed for force excitation systems were shown to be

capable of processing base excitation data under the condition that measured response data is transformed to the one relative to the base (Ref. 3). However, this type of transformation is inconvenient especially when many times of averaging with overlapping of the frame data are demanded in order to obtain a smooth spectrum. In this case, enormously large quantities of time-domain data must be stored in the computer memory before the FRF calculation is achieved. Hereafter a new method is derived based on the multi I/O random data analysis (Ref. 1).

The relative and absolute response acceleration vectors, $\underline{\ddot{X}}(t)$ and $\underline{\ddot{Y}}(t)$ have the following relation.

$$\underline{\ddot{X}}(t) = \underline{\ddot{Y}}(t) - \sum_{i=1}^3 \underline{I}_i \underline{\ddot{z}}_i(t) = \underline{\ddot{Y}}(t) - \underline{U} \underline{\ddot{Z}}(t) \quad (1)$$

\underline{z}_i refers to the base acceleration in the i direction, and \underline{I}_i is the direction vector ; $\underline{U} = (\underline{I}_1 \underline{I}_2 \underline{I}_3)$ and $\underline{\ddot{Z}}(t) = (\underline{\ddot{z}}_1 \underline{\ddot{z}}_2 \underline{\ddot{z}}_3)^t$. Fourier transform of equation (1) is,

$$\underline{\ddot{X}}(\omega) = \underline{\ddot{Y}}(\omega) - \underline{U} \underline{\ddot{Z}}(\omega) \quad (2)$$

Here, two kinds of FRF are defined as follows.

$$G_{j,i}(\omega) = E[\underline{\ddot{x}}_j(\omega)/\underline{\ddot{z}}_i(\omega)], \quad G_{j',i}(\omega) = E[\underline{\ddot{y}}_j(\omega)/\underline{\ddot{z}}_i(\omega)] \quad (3)$$

$E[]$ refers to the expected value. Suffixes i and j of $G_{j,i}(\omega)$ refer to the reference (or input) component and response (or output) component. $x_j(\omega)$, $y_j(\omega)$ and $\underline{\ddot{z}}_i(\omega)$ refer to the elements of $\underline{\ddot{X}}(\omega)$, $\underline{\ddot{Y}}(\omega)$ and $\underline{\ddot{Z}}(\omega)$. Using FRF matrix, $\underline{G}(\omega)$, which is composed of $G_{j,i}(\omega)$'s, relative response $\underline{\ddot{X}}(\omega)$ is expressed as follows.

$$\underline{\ddot{X}}(\omega) = \underline{G}(\omega) \underline{\ddot{Z}}(\omega) + \underline{N}(\omega) \quad (4)$$

where $\underline{N}(\omega)$ refers to the noise vector. In the microtremor measurement, most of the noise is considered to be the response to the wind forces. Therefore, it is reasonable to suppose that no relation exists between $\underline{N}(\omega)$ and $\underline{\ddot{Z}}(\omega)$.

$$\underline{S} \underline{N} \underline{\ddot{Z}}(\omega) = E[\underline{N}(\omega) \cdot \underline{\ddot{Z}}^H(\omega)] = \underline{0} \quad (5)$$

where \underline{S} refers to cross spectrum matrix and \underline{H} refers to the adjoint matrix. Substituting equations (2) and (4) into equation (5),

$$\underline{S} \underline{\ddot{Y}} \underline{\ddot{Z}}(\omega) - \underline{U} \underline{S} \underline{\ddot{Z}} \underline{\ddot{Z}}(\omega) - \underline{G}(\omega) \underline{S} \underline{\ddot{Z}} \underline{\ddot{Z}}(\omega) = \underline{0} \quad (6)$$

Consequently, the following equation is derived.

$$\underline{G}(\omega) = \underline{S} \underline{\ddot{Y}} \underline{\ddot{Z}}(\omega) \cdot \underline{S} \underline{\ddot{Z}} \underline{\ddot{Z}}^{-1}(\omega) - \underline{U} = \underline{G}'(\omega) - \underline{U}, \quad \text{where } \underline{G}'(\omega) = \underline{S} \underline{\ddot{Y}} \underline{\ddot{Z}}(\omega) \cdot \underline{S} \underline{\ddot{Z}} \underline{\ddot{Z}}^{-1}(\omega) \quad (7)$$

According to this equation, $\underline{G}(\omega)$ is processed by following two stages ; calculation of $\underline{G}'(\omega)$ in equation (7) directly using the measured data, $\underline{\ddot{Y}}(t)$ and $\underline{\ddot{Z}}(t)$; next, subtraction of constant matrix, \underline{U} , from $\underline{G}'(\omega)$. This method needs no subtraction of time history data in each frame, so, it is very convenient for data processing. Equation (7) implies the followings ; subtraction of 1 is needed for the FRF components which have the reference and response in the same direction ; the FRF components in which the directions of the reference and response are orthogonal, need no subtraction.

APPLICATION TO MICROTREMOR RECORDS OF BOILER PLANTS

Microtremor measurement Figure 1 shows the view of the boiler plant in a thermal power station. It is nearly 70 meters high. The boiler itself has an asymmetrical box type structure and weighs about 8000 tons. It is suspended from the roof girders of its supporting structure so as not to restrict its thermal expan-

sion in the vertical direction. In order to restrain its pendulum behavior in horizontal directions, stoppers are attached at certain points.

Microtremor measurements Microtremor records were measured during the periodic inspection of the boiler plant. Figure 2 shows the location of the sensors. Data was acquired in 8 levels including that of the base mat, and in each level, certain corners of the boiler and supporting structure were selected so as to specify the in-plane deformation of the structure using minimum number of sensors. At the locations 1 ~ 9, Seismometers are installed, too, but seismic records are not referred to in this paper.

Measured data is shown in Figures 3 and 4. The frequency spectra of the base mat show no peaks, but those of the structure have many peaks, which indicates the existence of many vibration modes in close proximity.

Multi-point random excitation methods demand low level of correlations between inputs (Ref. 1). Figure 5 shows the coherence spectrum between the two horizontal components of the base mat acceleration. The magnitude of coherence is below 0.1, which assures the validity of the application of this method.

Modal identification Table 1 shows the data processing conditions. The parametric study concerning the averaging number in the calculation of FRFs showed

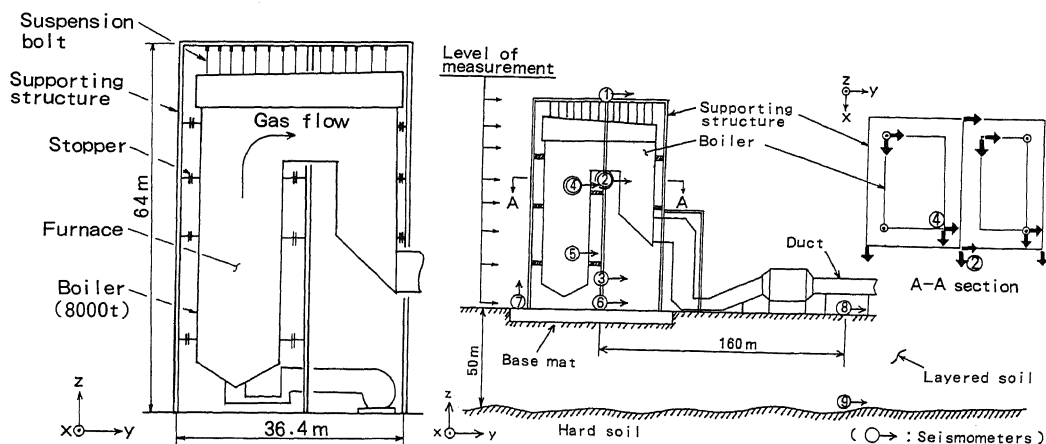


Figure 1 View of Boiler Plant Figure 2 Location of Vibrometers (Microtremor)

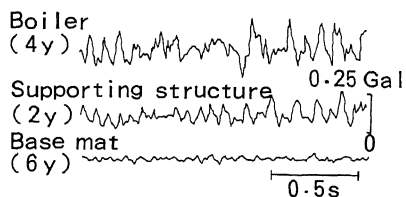


Figure 3 Microtremor Records

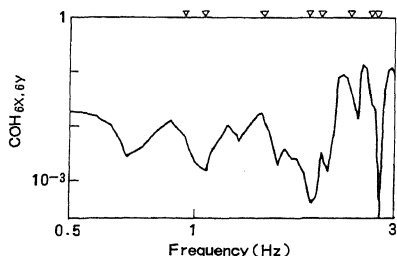


Figure 5 Correlation between Two Horizontal Components of Base Acceleration

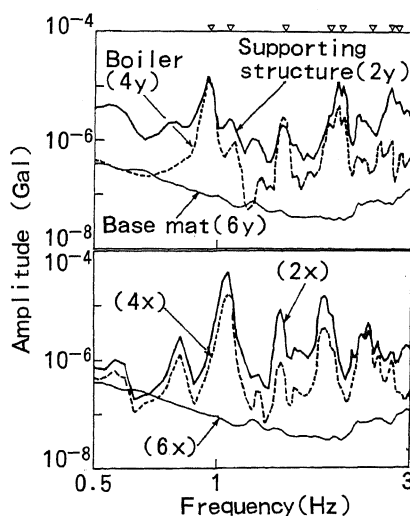


Figure 4 Frequency Spectra

that more than 200 times of averaging are needed to get the spectra smooth and stable. In averaging the spectrum, each frame time history data was overlapped 50 % in order to save the data. As to the polyreference curve-fitting method, vold's time-domain method (Ref. 2) was adopted because of its toughness against noise (Ref. 4). According to the FEM simulation of mode shapes, coupling is more remarkable between two horizontal directions than between the horizontal and vertical directions. Therefore, in the curve-fitting, two horizontal components of the base were used as the reference, and the vertical component was processed independent of them.

Figure 6 shows typical FRFs. They were acquired using the equation (7) in which two horizontal acceleration records of the base were used as inputs. In the upper two FRFs, reference and response have the same direction, but in the last one, reference and response are in the orthogonal direction. Table 2 shows the roots (natural frequencies and damping ratios) extracted by curve-fitting of these kinds of FRFs in many locations. The roots include pseudo-roots which have no physical meaning, so they must be eliminated. At first, the roots which have unreasonably large damping ratios were eliminated. In the following, a trial and error study was carried out. Using a random combination of roots, FRF was synthesized and compared with the measured one.

As a result of this study, 7 roots were evaluated as physical ones, which are shown in Table 2 without the * mark. The synthesized FRFs are shown in Figure 6 by the dashed lines. Comparison of these FRFs with the measured ones of solid lines show a good agreement with each other, which assures the validity of these roots. Corresponding mode shapes are shown in Figures 7 and 8 in order of their natural frequencies. Another mode shape was added which was extracted from the FRFs in the vertical direction. As a result, 8 modes of the boiler plant were identified.

Table 1 Data Processing Conditions

Items	Contents
Sampling freq.	64Hz
Frame size	2048 (32s)
Averaging no.	200
Overlapping factor	50%
Combination of $G_{j,i}(\omega)$ in Curve-fitting	1. $i = \ddot{X}_B, \ddot{Y}_B$ $j = n\ddot{X}, n\ddot{Y}, n\ddot{Z}$ 2. $i = \ddot{Z}_B$ $j = n\ddot{Z}$ ($n=1,2,\dots$: Location no.)

Table 2 Results of Curve-fitting

Estimated Root	Frequency	Damping	Amplitude	Phase
1	0.950	0.02688	2.29818E-02	-1.571
2 *	0.958	0.07288	0.72935	1.571
3 *	0.807	0.36782	0.32827	0.000
4 *	1.043	0.06473	0.18770	1.571
5	1.064	0.03108	1.4040	-1.571
6 *	1.373	0.07550	0.14680	-1.571
7 *	1.473	0.05627	2.57124E-02	1.571
8	1.496	0.04725	0.16220	1.571
9 *	1.603	0.04135	2.92275E-02	-1.571
10 *	1.878	0.04389	1.4506	1.571
11	1.894	0.03989	1.2921	-1.571
12	1.969	0.02552	0.12627	1.571
13 *	2.047	0.03709	0.15075	-1.571
14 *	2.106	0.16673	0.98820	1.571
15 *	2.262	0.06179	1.0403	1.571
16	2.343	0.02832	1.9044	-1.571
17 *	1.764	0.90515	1.9555	0.000
18 *	2.447	0.06170	1.1617	-1.571
19 *	2.624	0.07874	0.30803	1.571
20	2.655	0.03002	5.92437E-02	1.571
21 *	2.752	0.03307	0.76992	3.142
22 *	2.796	0.18007	0.23650	0.000

(*: Pseudo-root)

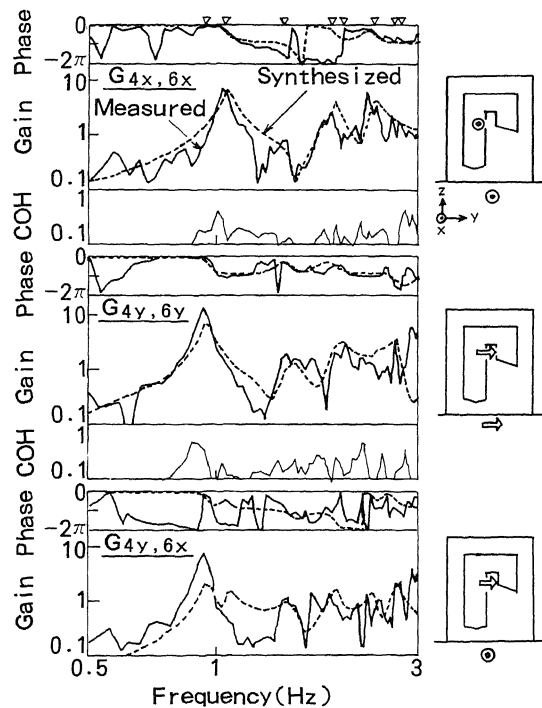


Figure 6 Frequency Response Functions

DISCUSSIONS

This chapter deals with the comparative study between the mode shapes of modal analysis and 8 lower mode shapes of FEM simulation. In order to achieve the quantitative evaluation of similarity between these two groups of mode shapes, an orthogonality check was carried out according to the equation, $\delta_{ij} = \underline{\psi}_i^t \underline{M} \underline{\phi}_j$, where $\underline{\psi}_i$ and $\underline{\phi}_j$ refer to the mode shapes of modal analysis and FEM, which are normalized using \underline{M} ; \underline{M} is mass matrix with lumped mass elements in the nodes which correspond to the location of measurement. In each group, mode shapes were numbered from 1 to 8 according to the magnitude of their natural frequencies, and δ_{ij} 's were calculated. In Table 3, underlined δ_{ij} 's show a large value which indicates a high degree of similarity and correspondence between $\underline{\psi}_i$ and $\underline{\phi}_j$.

According to these results, mode shapes of modal analysis and those of FEM were ordered in Figures 7 and 8. These mode shapes are divided into 4 types; three types of the mode shapes are specified by the remarkable deformation in each of X, Y and Z directions, and the last one is the twisting mode which is

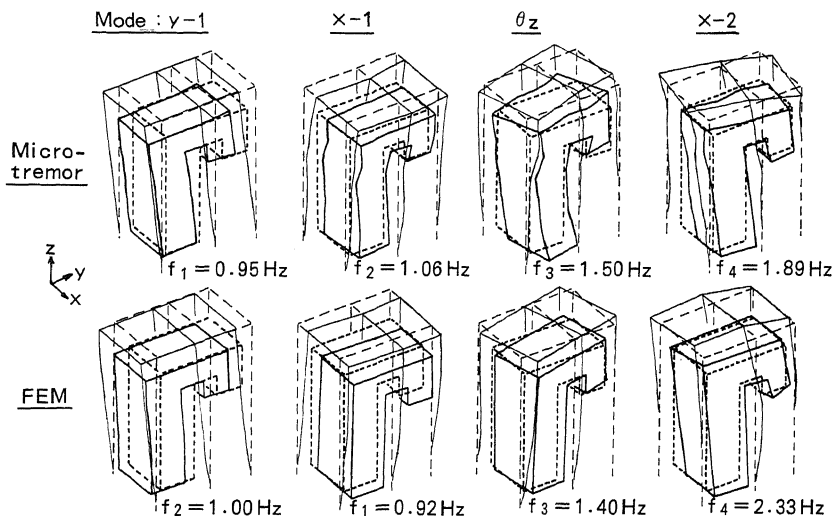


Figure 7 Comparison of Mode Shapes (1 ~ 4th)

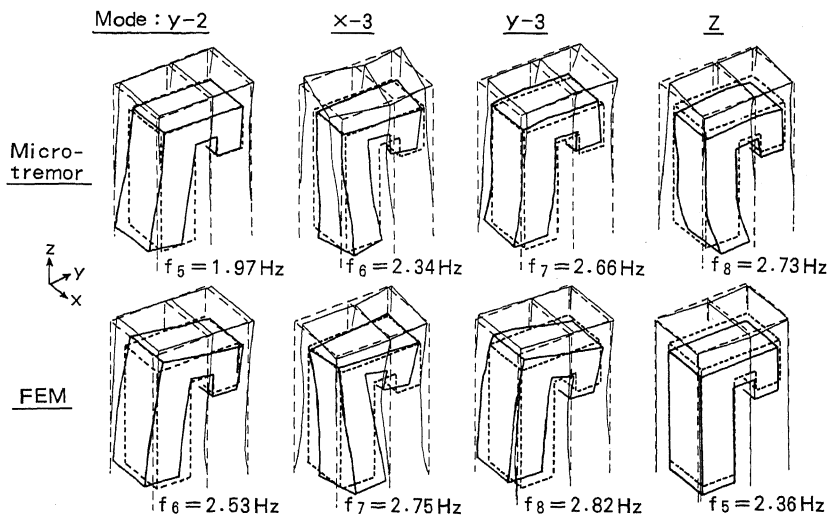


Figure 8 Comparison of Mode Shapes (5 ~ 8th)

referred to by ' θ_z '. This is a typical mode which is caused by the asymmetrical structure of the boiler plant. In each type, the mode shapes of modal analysis and those of FEM agree very well. But the values of underlined δ_{ij} 's in Table 3 tend to decrease in higher modes, which implies the increase of difference between the two groups of mode shapes. Lastly, the comparison between the natural frequencies of modal analysis and those of FEM show a relatively large difference in higher modes, but are in good agreement in the lower three modes which are dominant in the seismic response.

Table 3 Orthogonality between Mode Shapes

FEM	M/A	1	2	3	4	5	6	7	8
1	X-1	0.02	<u>0.95</u>	0.13	0.32	0.28	0.21	0.08	0.13
2	Y-1	<u>0.98</u>	0.12	0.14	0.01	0.11	0.01	0.12	0.14
3	θ_z	0.03	0.25	<u>0.75</u>	0.62	0.40	0.33	0.07	0.06
4	X-2	0.01	0.12	0.40	<u>0.59</u>	0.29	0.23	0.00	0.06
5	Z	0.01	0.10	0.01	0.04	0.04	0.17	0.17	<u>0.70</u>
6	Y-2	0.17	0.00	0.03	0.06	<u>0.63</u>	0.00	0.28	0.29
7	X-3	0.01	0.08	0.12	0.17	0.08	<u>0.71</u>	0.25	0.26
8	Y-3	0.01	0.02	0.03	0.04	0.50	0.02	<u>0.33</u>	0.25

CONCLUSIONS

Application method of multi-I/O experimental modal analysis to the base excitation data has been investigated. In this method, three directional components of the base acceleration and the response of the structure which is relative to the base, are utilized as input and output data.

This method has been applied to the microtremor records of the existing boiler plant and 8 modes were identified. They are in good correspondence with those of FEM. As a result, this type of modal analysis has proven to be an effective tool for the evaluation of seismic modeling.

ACKNOWLEDGMENT

The authors wish to thank Dr. Kohei Suzuki, Professor of Mechanical Engineering, Faculty of Technology in Tokyo Metropolitan University for his helpful suggestions for this study.

REFERENCES

1. Allemang, R.J., Rost, R.W., and Brown, D.L., "Dual Input Estimation of Frequency Response Functions for Automotive Structures, "SAE Paper 820193, (1982).
2. Vold, H., and Rocklin, G.T., "The Numerical Implementation of Multi-Input Modal Estimation Method for Mini-Computers, "Proceedings of 1st International Modal Analysis Conference, 542-548, (1982).
3. Nishida, E., Kasai, H., "Base Excitation Modeling by Modal Analysis and Its Application to Seismic Records of Boiler Plants, "Proceedings of the 1987 ASME PV&P Conference, PVP-Vol.127, 29-34, (1987).
4. Nagaike, M., Nagamatsu, A., and Yoshimura, T., "Research on Modal Analysis [4th Report, Multi Reference Curve-Fitting (Part 1)]," Transactions of the Japan Society of Mechanical Engineers (Series C), Vol. 51, No. 472, 3369-3376, (1985).